Breaking Waves on a dynamic Hele-Shaw Beach

Onno Bokhove[1], Bram van der Horn[2], Devaraj van der Meer[2],
Wout Zweers[4], and Anthony Thornton[3]
[1]Department of Applied Mathematics, E-mail: o.bokhove@utwente.nl
[2]Department of Applied Physics
[3]Departments of Applied Mathematics and Mechanical Engineering
University of Twente, The Netherlands.
[4]FabLab, Saxion Hogeschool, Enschede, The Netherlands

Abstract

We report the formation of quasi-steady beaches and dunes via breaking waves in our table-top 'Hele-Shaw' beach experiment. Breaking waves are generated by a wave maker, and zeolite particles act as sand. The tank is narrow, just over one-particle diameter wide, creating a quasi-2D set-up. Classical breaker types are observed on a time-scale of about a second. Beach formation under breakers occurs on a longer time-scale, and is a matter of minutes for a range of mono-chromatic wave frequencies. Alternating the wave maker motion between two frequencies generally leads to beach formation but occasionally to formation of a stable dune with water on either side. Finally, the Hele-Shaw configuration explored here experimentally lends itself to multi-scale modeling of beach dynamics.

1. Introduction

Surf-zone dynamics constitutes the dynamics of wave breaking, sediment and sand particle transport in the breaker zone at beaches. Beaches abound the world's coast-lines. Especially in coastal deltas and during storms from directions leading to the most hazardous sea conditions, beach and associated dune evolution strongly and intermittently change the coastal seascape. Understanding and prediction of this evolution will lead to the insight including which coastal communities are prone to flooding and erosional dangers by storm surges. While great advances have been made in hydro- and morpho-dynamics and coastal engineering (e.g., Soulsby 1997; Calantoni et al. 2004, 2006; Garnier et al. 2006, 2008, 2010), the laws of sand transport under breaking waves are still relatively poorly understood on a fundamental level. Accurate and manageable numerical techniques and tools predicting such transport dynamics are therefore still required. In the coastal situation, the number of sand particles involved dynamically is simply too large to allow direct numerical calculations of all grain and fluid motions, even though the Navier-Stokes equations for water and air motion and the continuum equations for grain interactions are in principle available. We have therefore raised the question whether it was possible to create a manageable, mathematical, modeling environment of beach dynamics with breaking waves and sand transport? Furthermore, can it be accompanied by a suitable laboratory experiment? Moreover, that environment has to be straightforward enough to permit brute force calculations of all hydro- and particle dynamics, as well as the construction and validation of a hierarchy of multi-scale models. Access to such multi-scale models of reduced conceptual and computational simplicity is required for further application to the reality of beach dynamics along our coasts.

The answer to the above question is as straightforward as cutting edge, and readily visualized: imagine oneself taking a giant's knife, making two cuts to isolate a slice of beach including sand and water, particle and wave motion, and placing it between two (glass) plates, if necessary after a suitable downscaling. The slice' separation is set to be a bit wider than one

particle diameter concerning mono-dispersed, relatively uniform particles. These confining, lateral boundaries can either be glass plates to allow good visualization, or even periodic walls in theoretical and computational models. A critique could be that our sliced-beach dynamics constitutes solely a virtual, mathematical or modeling reality. We therefore build a prototype to demonstrate the desired phenomenology in a table-top experiment. O.B. and W.Z. presented the Hele-Shaw beach dynamics life for the first time in a public art and science exhibition "Fluid Fascinations" of the Qua Art Qua Science Foundation (Bokhove et al. 2010). It was at the same time a celebration of the creative and visual spirit of the late Howell Peregrine, who was Professor in mathematics and in particular water waves, see Cooker (2010). This first set-up was 0.6m long, 0.3m high, and a few millimeter wide, with nearly spherical zeolite particles slightly smaller in diameter than this gap width. A vertical rod was driven horizontally to generate the waves, via a horizontal axel that was attached to a rotating disc on a drill. A sketch is given in Fig. 1. Our primary goal in the following is to demonstrate that the experiment functions. It can form beautiful beaches and dunes by strongly nonlinear, breaking waves.

The scope of this Hele-Shaw beach configuration is diverse: experimental, theoretical, and numerical. Firstly, the experiment is unique, because it focuses on particle motions under the heavy impact of breaking waves. Despite this violent dynamics, it allows easy visualization of the water surface, and individual particle motion due to the 1.1 particle diameter, lateral gap width. Lee et al. (2007) report experiments of one particle settling in a Hele-Shaw cell. They show that the dynamics remains quasi-two-dimensional for gap widths less than 1.1d (with d the particle diameter), while the dynamics becomes more three-dimensional for larger gap widths. Presently, we will mainly show novel results on beach and dune morphology arising in our Hele-Shaw beach set-up.

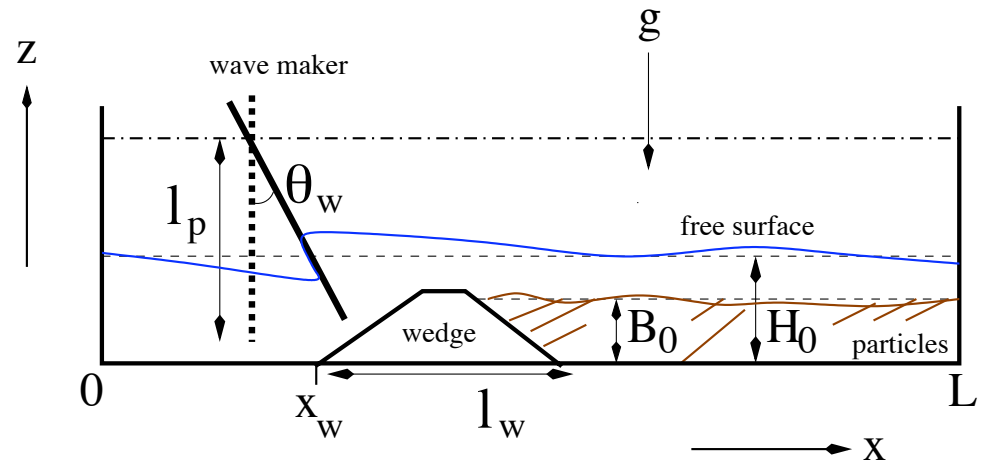

Figure 1. Sketch of the Hele-Shaw cell from the side with the wedge, waterline, particle bottom, and wave-maker rod in two positions outlined. The wedge holds particles away from the wave maker.

Secondly, it is this quasi-two-dimensional nature of our Hele-Shaw beach that is innovative. It allows excellent visualization and determination of fundamental water-particle and water-air interactions. It also permits a hierarchy of feasible mathematical and computational modeling, and enables a close comparison between experiment and modeling. The deficiencies of the set-up are manageable. They are due to the large damping caused by the close proximity of the lateral side-walls, and the strong influence of surface tension. But they can be bypassed because their effects are easily included in the models, and the phenomenology of beach and dune formation by strong wave breaking is still observed (due to the strong wave forcing and a calculated choice of the gap width). The impact of this amalgamation of experiments and modeling work lies in its potential to explore, validate and

analyze a hierarchy of models. One can employ brute-force models of nearly all particle and wave dynamics involved, and reduced models that do allow extension to three-dimensional beach dynamics along our coasts and associated forecast models. It therefore fills a nice niche for investigation of fundamental surf-zone morpho-dynamics under breaking waves in a stylistic, manageable research environment.

a)

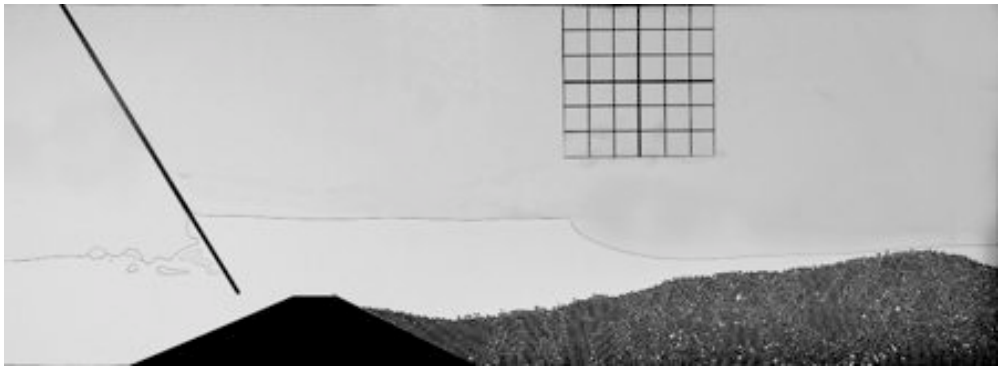

b)

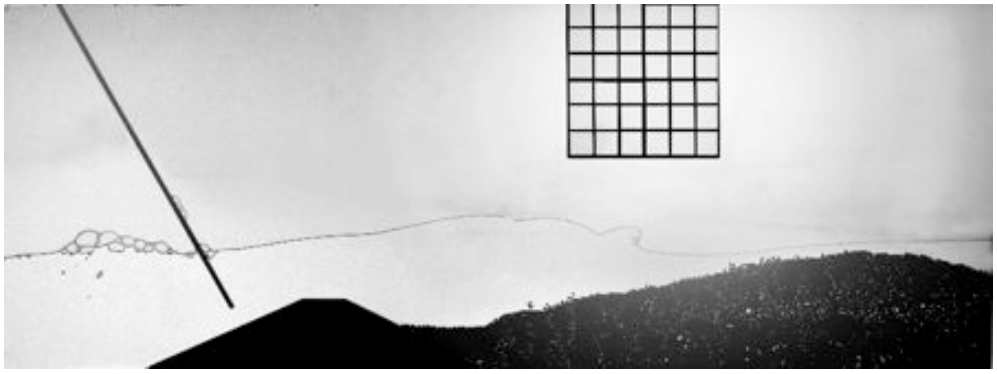

Figure 2. The Hele-Shaw beach table-top experiment consists of two vertical glass plates between which water and a monolayer of zeolite particles can move. The restricted lateral width (out of the page) enforces the movement of particles in a quasi two-dimensional plane (in the plane of the page), allowing easy tracking of all individual particles. The motor-driven wave-maker rod on the left of each image creates (breaking) waves leading to a net particle movement in the particle section to the right. That section is separated from the wave-maker region by a plexiglass wedge (darkened). The wavy waterline between water and air is visible as the black line. A 2x2 cm^2-grid gives some bearings. Two snapshots show a) a surging/spilling and b) a plunging breaker.

Finally, while the modeling allows a close comparison with the experiment, above and beyond it does permit a step-by-step extension to three dimensions. By replacing the fixed side walls by periodic boundary conditions the restrictions imposed by the side-wall friction and surface tension are completely removed. In addition, the gap width can be widened gradually to include more particles and, to some extent, this can also be done experimentally. In §2, mathematical and experimental aspects of the Hele-Shaw beach design are provided. In §3, we focus on beach and dune formation in our Hele-Shaw beach configuration, using water and the zeolite clay particles. Further exploration of different
fluids, different particle sizes and densities, and particle mixtures are left to the future, as discussed, in §4.

2. Design of the Hele-Shaw Beach

Our current Hele-Shaw beach set-up consists of two vertical glass plates 1.0m long, 0.3m high, separated by a gap of width 2l (with half-width l), and held in place by a wooden frame.

2.1 Role of Applied Mathematics

We have described how the Hele-Shaw beach configuration accommodates a combined experimental and numerical modeling approach. As we show in the following, applied mathematics was used to determine this gap width 2l. Breaking waves in shallow water are often modeled approximately as hydraulic jumps or bores, e.g., Lighthill (1978). In shallow-water models, such bores are discontinuities in the water depth h = h(x,t) and (mean) velocity u = u(x,t) as function of the horizontal coordinate x along the tank and time t. Consider the Hele-Shaw set-up for a prescribed beach floor b = b(x,t) relative to a horizontal datum z = 0 (the tank floor). Water motion is governed by the Navier-Stokes equations. After scaling these equations, damping due to viscosity in the lateral or y-direction is shown to dominate because the gap width is small relative to the planar velocity and length scales (horizontal and vertical x- and z-directions). This permits an approximation of the viscous momentum terms by ignoring terms with second-order x- and z-derivatives in the viscous terms.

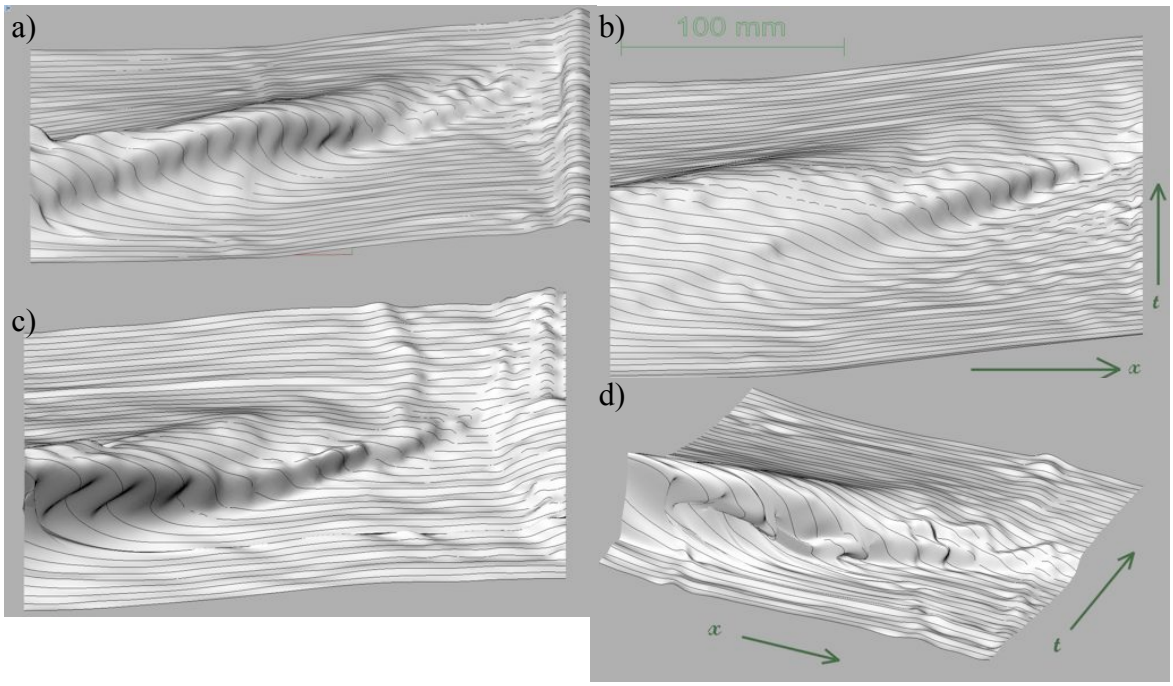

Figure 3. Rendered graphics of measured water surfaces versus space x (on the same scale) and time t are given for the (four) breaker types: a) spilling breaker (beach grains visible on right), b) surging breaker, c) collapsing breaker (beach grains visible on right and upper right), and d) plunging breaker. Time between frames is 0.02s.

It is tempting to assume a leading-order balance between pressure gradients and the remaining viscous terms to enforce *Hele-Shaw flow*. In the vertical plane this leads to

$$\tilde{u} = -\frac{\partial_x p}{\rho_0}\frac{(l^2 - y^2)}{2\nu} \quad \text{and} \quad \tilde{w} = -(\frac{\partial_z p}{\rho_0} + g)\frac{(l^2 - y^2)}{2\nu} \qquad (1)$$

with horizontal and vertical velocity components $\tilde{u}$ and $\tilde{w}$, pressure p, viscosity ν, constant acceleration of gravity g (pointing in the negative z-direction), density of water ρ_0, and derivative $\partial p / \partial x = \partial_x p$, etc. We compare the magnitudes of the planar pressure gradient or viscous terms $|\nabla_{xz} p|$ over the inertia terms $\rho_0 D\tilde{u} / Dt \sim 3\rho_0 \tilde{u}^2 / L$ Batchelor (1967),

using hydrostatic balance to estimate the pressure gradient (see below). We obtain

$$\frac{3\rho_0\tilde{u}^2}{L\,|\nabla_{xz}p|}=\frac{l^4\,|\nabla_{xz}p|}{3\rho_0\nu^2L}=\frac{l^4g\Delta h}{3\nu^2L^2}=\frac{l^4x10x(3x10^{-2})}{3x10^{-12}x(0.5)^2}\sim 0.1 \text{ to } 10 \qquad (2)$$

for l = 0.75 to 2mm. Consequently, we conclude that the inertial terms are equally important to the viscous ones. Hence, there is no pure Hele-Shaw flow but also inertial flow, despite the set-up's narrowness for a gap width of around 2mm.

Polhausen in Rosenhead (1963) substituted the quadratic approximation

$$\tilde{u}=\frac{3}{2}\bar{u}(l^2-y^2)/l^2 \quad \text{and} \qquad \tilde{w}=\frac{3}{2}\bar{w}(l^2-y^2)/l^2 \quad , \qquad (3)$$

based on the balance (1) into the Navier-Stokes equations and then laterally averaged these equations, using a width average $\bar{u}(x,z,t)=\int_{-l}^{l}\tilde{u}(x,y,z,t)dy/(2l)$, etc. Wilson and Duffy (1998) showed that approximation to be good in a similar yet different lubrication application, compared with numerical solutions of the Navier-Stokes equations. The width-averaging step is followed by the simplification that the average of products or functions is set to equal the product or function of the averages, thus neglecting (Reynolds) stress terms. The resulting system is a set of two-dimensional equations with linear momentum damping.

The subsequent step is to use the anisotropy in the horizontal and vertical directions and average over depth while using hydrostatic balance with kinematic free surface and bottom boundary conditions at the free surface z = h(x, t) + b(x, t) and bottom z = b(x, t). Integration of hydrostatic balance from a level z in the fluid to the free surface yields ρg(h(x,t)+b(x,t)-z); an estimate of the horizontal pressure gradient thus becomes ρΔh/L as used above in (2). After depth averaging and neglecting (Reynolds) stress terms, assuming a uniform flow profile over depth, shallow-water equations emerge

$$\partial_t(hu)+\partial_x(hu^2+gh^2/2)+(\gamma-1)hu\,\partial_x u=-gh\,\partial_x b-3\nu hu/l^2 \qquad (4a)$$

$$\partial_t h+\partial_x(hu)=0 \qquad (4b)$$

with a linear damping term in the momentum equation, γ = 6/5 arising from the width averaging, and $hu(x,t)=\int_{b}^{b+h}\bar{u}(x,z,t)dz$. These shallow-water equations are augmented with hydraulic jump and bore relations to allow for local, in one spatial dimension, point discontinuities in depth and velocity. We analyzed simulations of (4) for the approximate case γ = 1. A fixed mildly and uniformly sloping beach b~(x − x_0) was used on the right of x_0. On the left, a wave maker was modeled by prescribing the movement of a steep linear beach for $x < x_p < x_0$ around a pivoting point $x_p < x_0$ on the bottom. These simulations reveal that there is a threshold for which bores generated by the wave maker are strong enough to travel across a beach of about 0.5m when the gap width is 2l = 1.5mm and wave frequencies between 0.5–1.2Hz are applied. In contrast, for smaller gap widths 2l < 1.5mm the bores generated quickly die out due to the relatively strong, linear momentum damping in (4).

Given the availability of suitable zeolite particles of density ρ_0~2080±200 kg/m^3, and diameter d = 1.75±0.1mm. The gap width was thus chosen to be 2l = 2mm. Recall that this exactly gives the threshold ratio 2 l/d = 1.1 between the quasi-two-dimensional and three-dimensional fluid behavior observed by Lee et al. (2007) for the single-particle experiments in a Hele-Shaw cell.

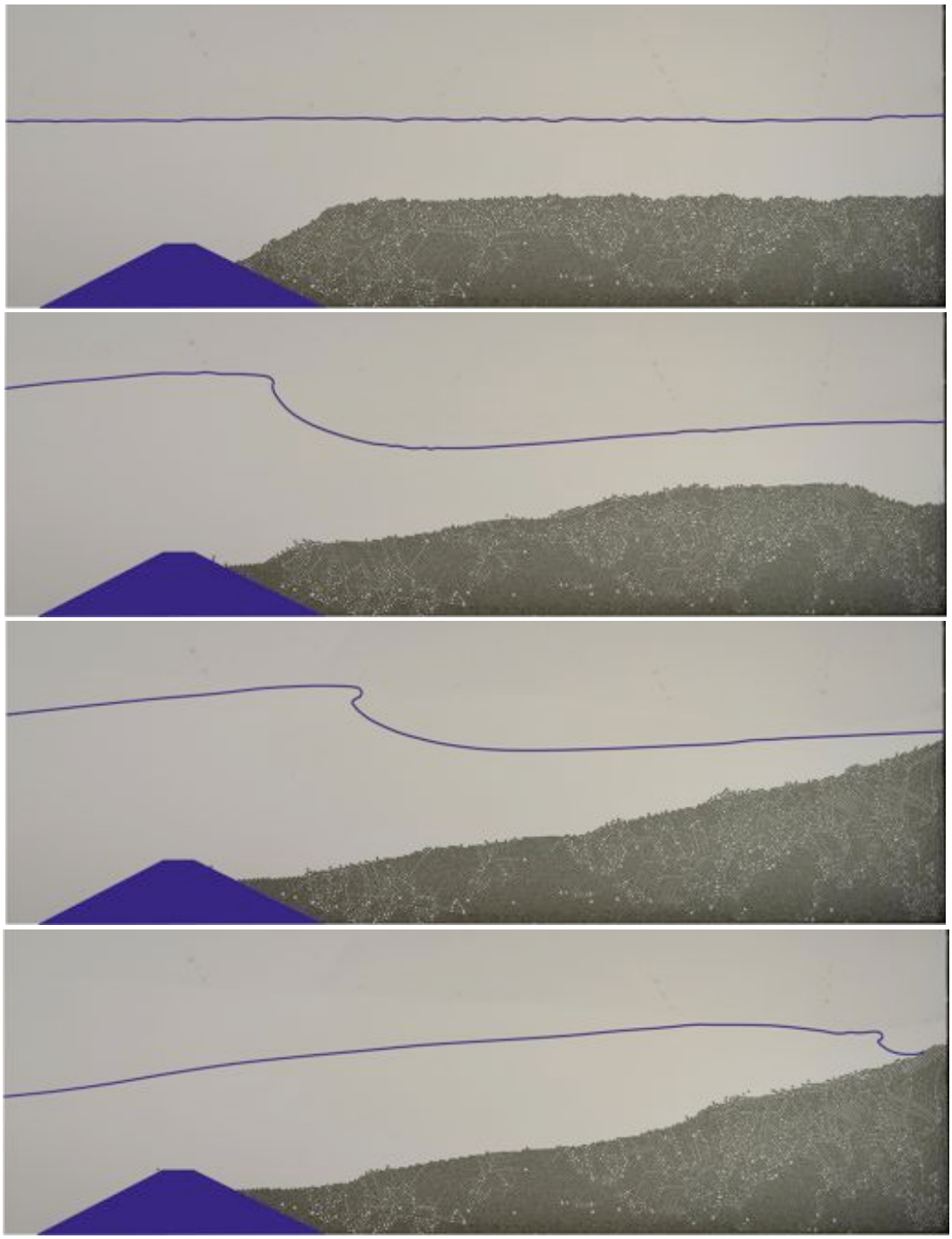

Figure 4. Profiles at t = 0,5,21:20,28:50 min (top to bottom) show beach formation under impact by monochromatic waves. Initially, waves move material from near the wedge to the shore. On longer time-scales a beach of nearly constant slope forms at the right wall, where a beach arises (last image).

2.2 Experimental Set-up

For the main results presented on this paper a second, longer Hele-Shaw beach set-up was constructed. Crucial experimental items are the spacers to separate the glass plates and the wave maker, and the choices of fluids and particles. We will discuss these in turn. Strips of spacers $2l = 2$mm wide are used along the bottom and vertical sides, and at three locations at the beginning, middle and end along the top of the glass plates. Screws along the bottom and three clamps along the top tighten the glass plates, ensuring the desired spacing to about ±0.05mm. The new set-up in principle also allows a gap width of 2 to 8mm. The wave maker consists of two joined, circular welding rods, each one 1.5mm in diameter. They form a pendulum with its pivoting point connected magnetically to a metal bearing attached to two aluminum U-profiles just above the glass plates. It is driven by a horizontal, adjustable axel with screw thread, connected on the side to a reassembled printer-driver. This driver can be programmed in the frequency range 0.5 and 1.2 Hz and for a range of amplitudes. The open-source electronic platform Arduino was used to preprogram the driver. Four switches allowed frequencies to change manually without interruption during operation. Such was needed in the subtle hysteretic process of dune or island formation, which we will describe shortly. We measured the wave-maker motion to establish the extent to which this input matches the output. For a programmed, monochromatic wave frequency the output signal is close to a sine wave, and the error in the smallest wave frequency is 0.50 ± 0.01 Hz. Demineralized water is used and nearly spherical, zeolite, clay particles of (1.75 ± 0.1) mm diameter. It is important to keep the wave tank clean, for which we use white spirits, traces of which are removed by flushing with ample demineralized water. The set-up is seal and hence watertight. Fluids are added via a funnel attached to an exit valve in a bottom corner of the tank, which also serves to remove fluids and particles after a series of experiments. It is important to clean and empty the set-up carefully, and avoid pollution by settling dust or algae growth. A symmetric, plexiglass wedge with a flat base of length 0.22m, height 0.05m and flat top of length 0.02m positioned at $x_w \sim 0.31$m off the bottom left corner, separates the wave-maker region from the region with grains. That is necessary to avoid the wave maker coming into direct contact with the particles, causing grinding of the particles or the wave maker ceasing up. The wave maker rod in vertical position extends to about 0.02m off the bottom and its length from the pivot point is $l_p = 0.331$m. A sketch is given in Fig. 1. Two snapshots in Fig. 2 zoom in on the wavy air-water interface and water-particle boundary, but also show the wave maker and plexiglass wedge.

3. Experimental Results

The idea is that the Hele-Shaw beach experiments capture key elements of the complex three-dimensional problem of wave breaking within a quasi-two-dimensional world. While we will mostly focus on time-dependent beach morphology caused by wave impact on the longer time-scales of minutes, we will briefly summarize the wave action forcing the morphological changes on the shorter time-scale of the wave. It is about one second. Nearly all breaking-wave types classified in the review article of Peregrine (1983) are observed, including spilling, plunging, collapsing and surging breakers. For a spilling breaker, white water at the wave crest spills down the front face sometimes with the projection of a small jet. For a plunging breaker, the wave front overturns and a prominent jet falls at the base of the wave causing a large jet. For a collapsing breaker, the lower portion of the wave's front face overturns and then behaves like a plunging breaker; this breaker type is hardly seen in our experiment and perhaps remotely recognizable in Fig. 3c). For a surging breaker, a significant disturbance in an otherwise smooth profile occurs only near the moving shoreline. A shore break is a small variation on a surging breaker in which the whole face from through to crest becomes vertical with little to no water in front. The sequences involved for all wave types

are unraveled in space-time renderings of the free surface in Fig. 3.

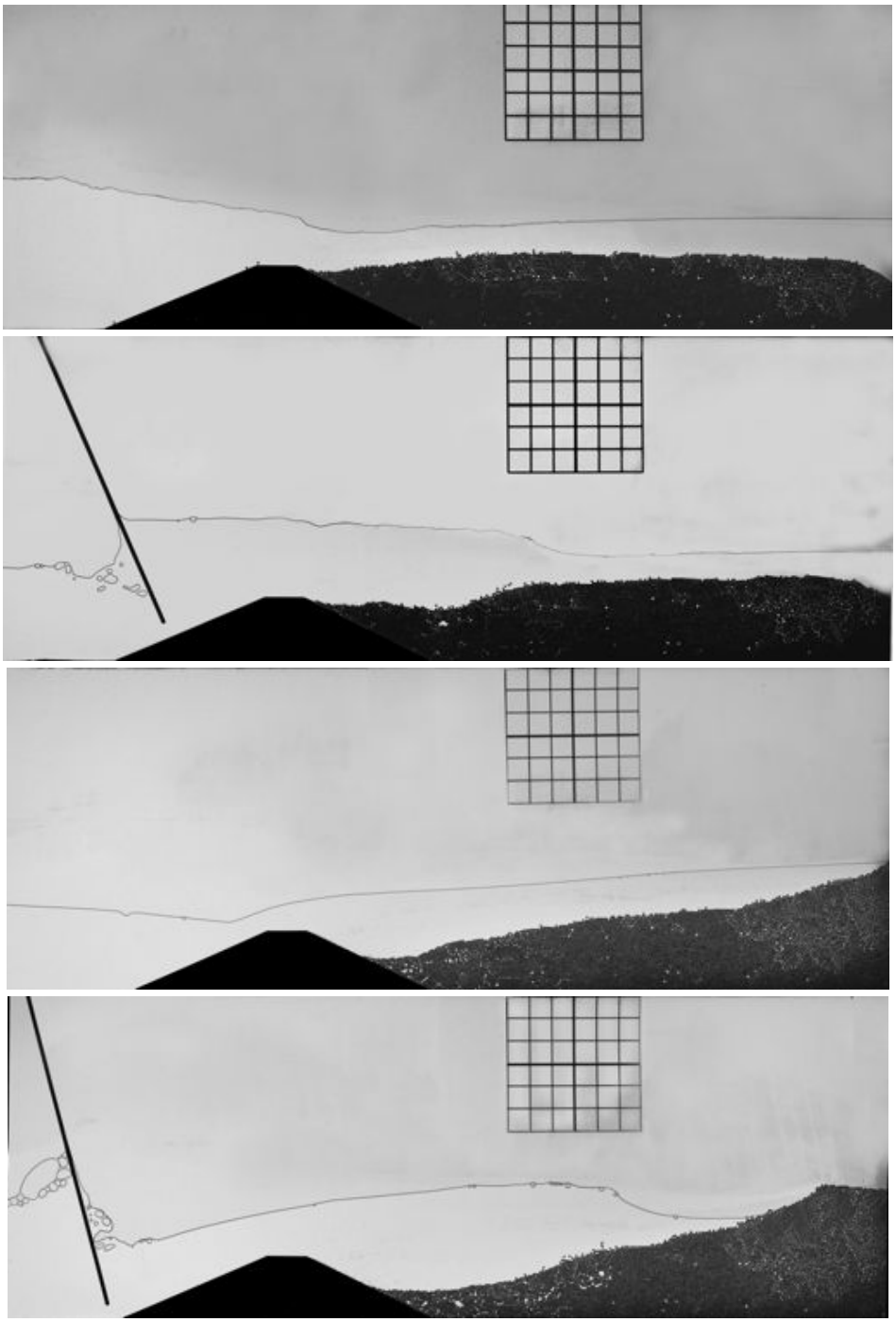

Figure 5. Profiles (top to bottom) are shown of beach formation under wave impact for two wave frequencies, changed intermittently, at t = 0, 2.5, 10.5, 25.5min.

3.1 Beach Creation

Beach formation by breaking waves is observed in our Hele-Shaw cell. First, we investigate for which monochromatic, wave-maker frequencies in the range f = [0.5, 1.5]Hz beaches are formed. We start from a rest state with a nearly flat bed (see Fig. 4 top panel). The dynamics also depends on the wave-maker amplitude θ_w and the initial water depth H_0 above the flat bed. In principle also the initial thickness B_0 of the bed is relevant but we assume it to be deep enough. The frequency was increased by 0.1 Hz and between [0.6, 1.2]

Hz, inclusive, and beaches were formed within minutes. Two time indicators for beach formation are used: the first time T_d for which the beach falls dry in a wave cycle, and a time T_f for which the final profile is in quasi-steady state for about 10 wave cycles. Beach formation was fastest for f = 1 Hz, in about T_d = 23min. Snapshots of the evolution of beach dynamics are shown in Fig. 4 for f = 1Hz, H_0=0.130m, B_0 = 0.080m, x_w =0.370, $\theta_w = 18.6^o$ (new 1 m-long cell). The wave maker arm has length l_p =0.331m and lies about 5mm off the bottom when vertical. Profiles are show at times t = 0,5,21:20,28:50min. A steady state was reach about time T_f = 29min.

3.2 Island or Dune Formation

Dune formation is defined as the formation of a final quasi-steady state beach profile with an island or dune separated from the mainland wall by a pool of quiescent water behind the dune. We start again from a state of rest with nearly flat bed. We first encountered dune formation starting from a very rough flat bed by educated changes between wave-maker frequencies f = 0.6 and 0.9 Hz. That way we have created dune formation occasionally among some failed attempts. A failed attempt is shown in Fig. 5, in which the frequency pattern has been f=0.6 Hz for t=[1, 3], [11,13:30], [22, 23] and f = 0.9 Hz for t = [4, 11], [13:30, 22], [23, 30] min. with smooth transitions from one interval to another. It led to a single beach with a characteristic, landmark cliff in the final state. In contrast, dune formation occurred for the following frequency patterns: f =0.6 Hz for t=[0, 3], [10, 12:40], [21, 22] and f = 0.9 Hz for t=[3, 10], [12:40, 21], [22, …] min. with abrupt changes between the two frequencies via a transition period of a few seconds in which wave maker motion stopped (H_0 = 0.03m, B_0 = 0.099 m). The restart caused a freak wave to occur when the wave-maker settled to its new frequency. Cliff formation on the sea-side of the dune occurred at t = 37 min., as seen in Fig. 6. We have not been able to repeat dune formation for this exact frequency pattern, perhaps because we reprogrammed the wave-maker routine to allow for smooth frequency transitions. Dune formation appears to occur when freak waves have caused a catastrophic change in beach morphology or when the initial bed profile is rather rough due to precursory wave impacts. Hence, dune formation can be hysteretic. For sufficiently small $(H_0 - B_0)>0.01$m, however, we could recently also find dune formation in the middle of the sandy section for monochromatic wave-maker frequencies. Wave energy then quickly dissipates due to wave breaking near the edge of the shallow sea.

4. Discussion

We have demonstrated the rich phenomenology of particle dynamics by breaking waves in the Hele-Shaw beach configuration we invented. It lends itself readily for fundamental experimental, numerical and mathematical research. Experimentally, one can explore the rich phenomenology of beach dynamics by recording beach and dune profiles as function of wave frequencies, domain shape, water depth, liquid and particle properties in space and time. Numerically, one can simulate dynamics in a brute-force manner and use such simulations as benchmarks, because the quasi-two-dimensional framework ensures the computation time to be manageable. Combined particle and smoothed particle (hydro)dynamics calculations therefore become feasible. Mathematically, the geometry of the set-up allows us to derive, compare and validate a hierarchy of multi-scale models with closure laws. Furthermore, the end members of this hierarchy will permit extension to more three-dimensional dynamics, in terms of complexity and computational demands. The beauty of the Hele-Shaw configuration is that an entire research methodology becomes feasible for complex processes of beach evolution induced by wave breaking, because its essence is captured in a quasi-two-dimensional setting.

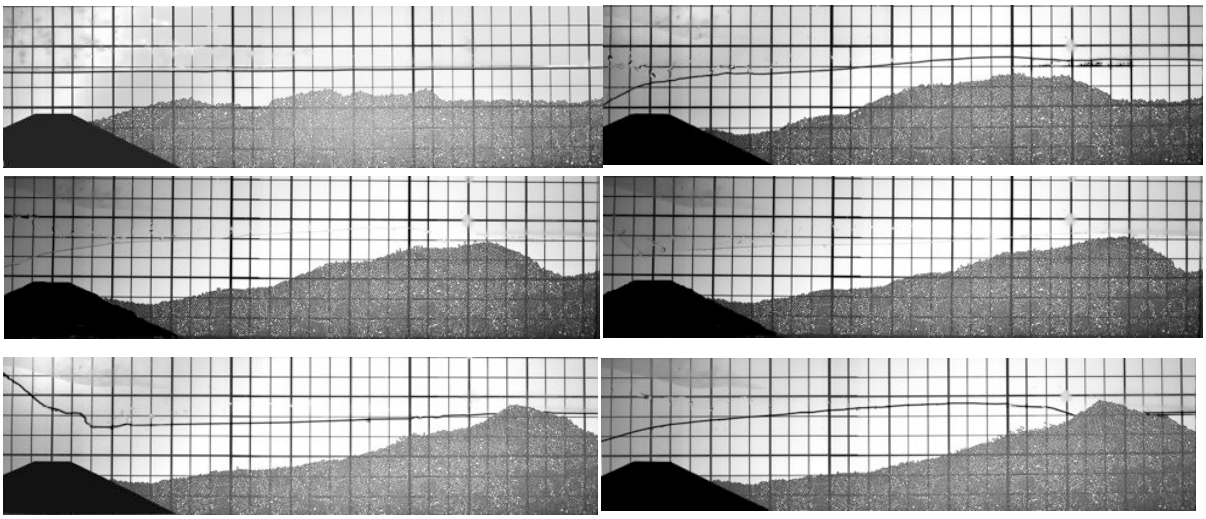

Figure 6. Snapshots are shown at t = 0, 9, 18, 27, 36 and 45 min. (top to bottom) showing dune formation. A waterline separates water from air. We intermittently change wave frequencies between 0.6 and 0.9 Hz. Finally, a quiescent lake emerges behind the dune (last image).

Acknowledgements

It is a pleasure to acknowledge the "Stichting Free Flow Foundation" for financial and the "Stichting Qua Art Qua Science" for moral support (Bokhove et al. 2010).

References

Batchelor, G.K. (1967) *An Introduction to Fluid Dynamics.* Cambridge University Press. 635 pp.

Bokhove, O., Zwart, V. and Haveman, M.J. (2010) *Fluid Fascinations.* Publication of Stichting Qua Art Qua Science, University of Twente, Enschede, The Netherlands.

Calantoni, J., Holland, K.T. and Drake, T.G. (2004) Modelling sheet-flow sediment transport in wave-bottom boundary layers using discrete-element modelling. *Phil. Trans. Roy. Soc. Lond. A* **362**,1987–2001.

Calantoni, J. Puleo, J.A. and Holland, K.T. (2006) Simulation of sediment motions using a discrete particle model in the inner surf and swash-zones. *Cont. Shelf Res.* **26**, 1987–2001.

Cooker, M. (2010) A commemoration of Howell Peregrine 1938-2007. *J. Eng. Math.* **67**, 1–9.

Garnier, R. Calvete, D., Falques, A. and Cabelleria, M. (2006) Generation and nonlinear evolution of shoreoblique/ transverse sand bars. *J. Fluid Mech.* **567**, 327–360.

Garnier, R. Calvete, D., Falques, A. and Dodd, N. (2008) Modelling the formation and the long-term behavior of rip channel systems from the deformation of a longshore bar. *J. Geophys. Res.* **113**, C07053.

Garnier, R., Dodd, N., Falquez, A. and Calvete, D. (2010) Mechanisms controlling crescentic bar amplitude. *J. Geophys*. Res. **115**, F02007.

Lighthill, J. (1978) *Waves in Fluids.* Cambridge University Press, 504 pp.

Lee, A.T., Ramos, E. and Swinney, H.L. (2007) Sedimenting sphere in a variable-gap Hele-Shaw cell. *J. Fluid Mech.* **586**, 449-464.

Peregrine, D.H. (1983) Breaking waves on beaches. *Ann. Rev. Fluid Mech.* **15**, 149–178.

Rosenhead, L. (ed.) (1963) *Boundary Layer Theory.* University Press Oxford. 688 pp.

Soulsby, R. (1997) *Dynamics of Marine Sands.* In: HR Wallingford. Thomas Telford. 249 pp.

Wilson, S.K. and Duffy, B.R. (1998) On lubrication with comparable viscous and inertia forces. *Q.J. Mech. Appl. Math.* **51**, 105–124.